Computers and Structures 127 (2013) 29–38

Contents lists available at SciVerse ScienceDirect

Computers and Structures

journal homepage: www.elsevier.com/locate/compstruc

On the consistent formulation of torques in a rotationless framework for multibody dynamics

P. Betsch *, N. Sänger

University of Siegen, Paul-Bonatz-Straße 9-11, 57068 Siegen, Germany

ARTICLE INFO

Article history:
Received 9 June 2012
Accepted 8 October 2012
Available online 17 November 2012

Keywords:
Natural coordinates
Cosserat solids
Flexible multibody dynamics
Structure-preserving time integration
Energy–momentum method

ABSTRACT

A rotationless formulation of flexible multibody dynamics in terms of natural coordinates is considered. Since natural coordinates do not comprise rotational parameters, the consistent formulation and numerical discretization of actuating torques becomes an issue. In particular, the straightforward time discretization of the forces conjugate to natural coordinates may lead to a significant violation of the balance law for angular momentum. The present work shows that the theory of Cosserat points paves the way for the consistent incorporation and discretization of actuating torques. The newly proposed method adds to the energy–momentum consistent numerical integration of flexible multibody dynamics.

1. Introduction

The present work deals with a rotationless description of flexible multibody dynamics that circumvents the use of rotational parameters (Betsch et al. [1,2]). The present approach relies on the canonical embedding of the rotation group into a nine-dimensional linear space. Accordingly, the orientation of a rigid body in space is characterized by nine direction cosines which define a director triad fixed at the rigid body and moving with it

A similar approach can be applied to Cosserat solids such as shear deformable beams and shells. In Betsch and Steinmann [4,5] and Betsch and Sänger [6] the rotationless formulation and numerical discretization of geometrically exact Cosserat beams and shells is treated. The advantages of Cosserat solids for the description of flexible multibody systems are emphasized as well in the works by Géradin and Cardona [7], Ibrahimbegović and Mamouri [8], and Bauchau [9].

In this connection, structure-preserving time-stepping methods such as energy–momentum schemes are considered important due to their enhanced numerical stability and robustness, see Géradin and Cardona [7, Chapter 12], Ibrahimbegović et al. [10], Bathe [11], and Bauchau [9, Chapter 17]. It is worth noting that the rotationless formulation of flexible multibody dynamics makes possible the straightforward design of structure-preserving time-stepping schemes such as energy–momentum schemes and momentum-symplectic integrators (Leyendecker et al. [12] and Betsch et al. [13]).

On the other hand the nonstandard rotationless description of rigid bodies and Cosserat solids requires some care concerning the consistent application of actuating torques. The present rigid body

coordinates are comprised of Cartesian components of unit vectors and Cartesian coordinates. It is worth noting that our specific choice of natural coordinates (Betsch and Steinmann [3]) has its roots in theoretical mechanics (Saletan and Cromer [15, Chapter 5]).

Using natural coordinates, the application of external torques becomes an issue since conjugate rotational parameters are not available. One way to resolve this issue is the introduction of additional coordinates which are appended to the natural coordinates via specific algebraic constraints (García de Jalón [14] and Uhlar and Betsch [16]).

Alternatively, the redundant forces conjugate to the natural coordinates can be used to take into account the action of external torques. In the present work we focus on this approach. We show that the straightforward time discretization of the forces conjugate to natural coordinates may lead to a significant violation of the balance law for angular momentum. To remedy the situation we recast the rotationless formulation of rigid bodies in terms of skew

* Corresponding author. Address: Department of Mechanical Engineering, University of Siegen, Paul-Bonatz-Straße 9-11, 57068 Siegen, Germany.

E-mail addresses: peter.betsch@uni-siegen.de (P. Betsch), saenger@imr.mb.uni-siegen.de (N. Sänger).

0045-7949
http://dx.doi.org/10.1016/j.compstruc.2012.10.005

coordinates. This approach paves the way for the consistent time discretization of the equations of motion. It is worth noting that our newly proposed method has been guided by the close connection between natural coordinates and the theory of Cosserat points (Rubin [17]).

An outline of the rest of the paper is as follows. In Section 2 the equations of motion providing the framework for the present description of flexible multibody systems are summarized. The formulation of rigid body dynamics in terms of natural coordinates is dealt with in Section 3. The extension of the present approach to multibody dynamics is illustrated in Section 4 with the formulation of lower kinematic pairs. After a summary of the main features of the present approach in Section 5, the structure-preserving discretization in time is dealt with in Section 6. To demonstrate the capability of the proposed method two numerical examples are presented in Section 7. Eventually, conclusions are drawn in Section 8.

2. Equations of motion

We start with the equations of motion pertaining to a finite-dimensional mechanical system subject to holonomic constraints. From the outset we confine ourselves to mechanical systems whose kinetic energy can be written as

$$T(\dot{\boldsymbol{q}}) = \frac{1}{2}\dot{\boldsymbol{q}} \cdot \boldsymbol{M}\dot{\boldsymbol{q}} \tag{1}$$

Here, $\boldsymbol{q} \in \mathbb{R}^n$ is the vector of redundant coordinates and a superposed dot denotes the derivative with respect to time. Moreover $\boldsymbol{M} \in \mathbb{R}^{n\times n}$ is a **constant** mass matrix. As has been outlined in the Introduction a constant mass matrix is a consequence of the use of natural coordinates for the description of spatial multibody systems. The equations of motion pertaining to the discrete mechanical systems of interest can be written in variational form

$$G^{\delta} = \delta\boldsymbol{q} \cdot \left(\boldsymbol{M}\ddot{\boldsymbol{q}} + \sum_{l=1}^{m} \lambda^l \nabla g_l(\boldsymbol{q}) - \boldsymbol{F} \right) = 0 \tag{2}$$

which has to be satisfied for arbitrary $\delta\boldsymbol{q} \in \mathbb{R}^n$. The last equation has to be supplemented with algebraic constraint equations $g_l(\boldsymbol{q}) = 0$, $1 \leqslant l \leqslant m$. The associated constraint forces assume the form $\sum \lambda^l \nabla g_l(\boldsymbol{q})$, where λ^l are Lagrange multipliers. The last term in (2) accounts for external forcing. For simplicity of exposition we do not distinguish between forces that can be derived from potentials and nonpotential forces. Note, however, that we may replace $\boldsymbol{F} \in \mathbb{R}^n$ in (2) with

$$\boldsymbol{F} \rightarrow \boldsymbol{F} - \nabla U(\boldsymbol{q}) \tag{3}$$

Then, the potential forces are derived from a potential function $U(\boldsymbol{q})$, and the nonpotential forces are contained in $\boldsymbol{F}$. Due to the presence of algebraic constraints the equations of motion assume the form of differential–algebraic equations (*DAEs*). The configuration space of the constrained mechanical systems under consideration is defined by

$$\mathrm{Q} = \{\boldsymbol{q} \in \mathbb{R}^n | g_l(\boldsymbol{q}) = 0,\ 1 \leqslant l \leqslant m\} \tag{4}$$

Throughout this work we assume that the constraints are independent. Consequently, the vectors $\nabla g_l(\boldsymbol{q}) \in \mathbb{R}^n$ are linearly independent for $\boldsymbol{q} \in \mathrm{Q}$. Due to the presence of m geometric constraints the discrete mechanical system under consideration has $n - m$ degrees of freedom. Admissible variations $\delta\boldsymbol{q}$ have to belong to the tangent space to Q at $\boldsymbol{q} \in \mathrm{Q}$ given by

$$T_q\mathrm{Q} = \{\boldsymbol{v} \in \mathbb{R}^n | \nabla g_l(\boldsymbol{q}) \cdot \boldsymbol{v} = 0,\ 1 \leqslant l \leqslant m\} \tag{5}$$

Remark 2.1. The variational form (2) of the equations of motion is equivalent to Lagrange's equations (of the first kind), which may be linked to the Lagrange-d'Alembert principle

$$\delta \int_{t_0}^{t_N} \left(T(\dot{\boldsymbol{q}}) - \sum_{l=1}^{m} \lambda^l g_l(\boldsymbol{q}) \right) dt + \int_{t_0}^{t_N} \delta\boldsymbol{q} \cdot \boldsymbol{F}\, dt = 0 \tag{6}$$

The Lagrange-d'Alembert principle can be viewed as an extension of Hamilton's principle to account for external forcing, see Marsden and Ratiu [18].

Remark 2.2. In the above description $\boldsymbol{F} \in \mathbb{R}^n$ is loosely termed 'external force vector'. In a multibody system formulated in terms of natural coordinates each individual component of F refers to a specific rigid body (see Section 3 for further details) or a specific node of the finite element discretization of a flexible beam or shell component. Thus the action of joint-forces can be represented by components of $\boldsymbol{F}$, although joint-forces are internal forces (or torques) from the multibody system perspective. If the external force components are to represent joint-forces Newton's third (or action-reaction) law has to be obeyed.

3. Rigid body dynamics in terms of skew coordinates

We next present a reformulation of the rotationless formulation of rigid body dynamics (Betsch and Steinmann [3] and Saletan and Cromer [15, Chapter 5]). The original version of the rotationless formulation relies on the assumption of an orthonormal director frame. The orthonormality of the director frame is related to the rigid body assumption and enforced by algebraic constraints. However, the direct discretization of the DAEs typically relaxes the constraints to discrete points in time (see Section 6). Correspondingly, in the discrete setting the orthonormality of the director frame is confined to discrete (or nodal) points in time. This implies that convex combinations of the nodal directors in the discrete setting represent base vectors that are in general neither of unit length nor mutually orthogonal. This deficiency (or more specifically, the discretization error) can be taken into account by introducing skew coordinates from the outset. In particular, the use of skew coordinates turns out to be beneficial to the formulation and consistent numerical discretization of external torques.

In the following we use convected coordinates θ^i to label a material point belonging to the rigid body (Fig. 1). The position of a material point at time t can be described by

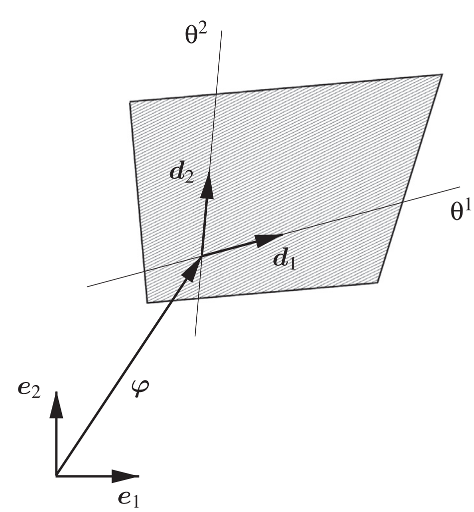

Fig. 1. Planar sketch of the rigid body.

$$\boldsymbol{x} = \boldsymbol{\chi}(\theta^i, t) = \boldsymbol{\varphi}(t) + \theta^i \boldsymbol{d}_i(t) \tag{7}$$

where $\boldsymbol{\varphi} = \varphi^i \boldsymbol{e}_i$ is a reference point fixed in the body, $\boldsymbol{d}_i = (\boldsymbol{e}^j \cdot \boldsymbol{d}_i)\boldsymbol{e}_j$ are director vectors, and $\boldsymbol{e}_i = \boldsymbol{e}^i$ are orthonormal base vectors fixed in space.[1] Due to the kinematic relation (7), the covariant base vectors coincide with the directors, i.e. $\boldsymbol{g}_i = \partial \boldsymbol{x}/\partial \theta^i = \boldsymbol{d}_i$. For the time being the directors $\boldsymbol{d}_i$ can be regarded as base vectors that need not be of unit length nor mutually orthogonal. As mentioned before, the present use of skew coordinates can be viewed as generalization of previous rigid body formulations relying on the components of the direction-cosine matrix. This generalization turns out to be advantageous for the discretization in time dealt with in Section 6. We further assume

$$d^{\frac{1}{2}} = \boldsymbol{d}_1 \cdot (\boldsymbol{d}_2 \times \boldsymbol{d}_3) > 0 \tag{8}$$

Additional constraints will be imposed in the sequel to enforce the rigid body assumption. In addition to the covariant base vectors we introduce contravariant base vectors

$$\boldsymbol{d}^i = d^{-\frac{1}{2}}(\boldsymbol{d}_j \times \boldsymbol{d}_k) \tag{9}$$

for even permutations of the indices (i,j,k). Consequently, $\boldsymbol{d}^i \cdot \boldsymbol{d}_j = \delta^i_j$, the Kronecker delta. In the following the contravariant base vectors $\boldsymbol{d}^i$ will be called contravariant directors.

The kinematic relationship (7) indicates that the configuration of a single rigid body can be described by $n = 12$ coordinates that can be arranged in the configuration vector

$$\boldsymbol{q} = \begin{bmatrix} \boldsymbol{\varphi} \\ \boldsymbol{d}_1 \\ \boldsymbol{d}_2 \\ \boldsymbol{d}_3 \end{bmatrix} \tag{10}$$

To calculate the mass matrix $\boldsymbol{M} \in \mathbb{R}^{12\times 12}$ we consider the continuum expression for the kinetic energy

$$T = \frac{1}{2}\int_{\mathcal{B}_0} \rho_0 \boldsymbol{v} \cdot \boldsymbol{v} D^{\frac{1}{2}} d^3\theta \tag{11}$$

where $\mathcal{B}_0$ denotes the reference configuration of the body at time $t = 0$. Correspondingly, $\rho_0 : \mathcal{B}_0 \to \mathbb{R}_+$ is the reference mass density and $D = d(0)$, where $d(t)$ is given by (8). The material velocity $\boldsymbol{v}$ can be calculated from (7):

$$\boldsymbol{v} = \frac{\partial}{\partial t}\boldsymbol{\chi}(\theta^i, t) = \boldsymbol{v}_\varphi(t) + \theta^i \boldsymbol{v}_i(t) \tag{12}$$

Here $\boldsymbol{v}_\varphi = \dot{\boldsymbol{\varphi}}$ is the velocity of the point of reference and $\boldsymbol{v}_i = \dot{\boldsymbol{d}}_i$ will be referred to as director velocities. Inserting the last equation into (11) a straightforward calculation yields the kinetic energy in the form

$$T = \frac{1}{2} M_\varphi \boldsymbol{v}_\varphi \cdot \boldsymbol{v}_\varphi + e^i \boldsymbol{v}_\varphi \cdot \boldsymbol{v}_i + \frac{1}{2} E^{ij} \boldsymbol{v}_i \cdot \boldsymbol{v}_j \tag{13}$$

In the last equation the total mass M_φ and the director inertia coefficients e^i, E^{ij} are defined by

$$\begin{aligned} M_\varphi &= \int_{\mathcal{B}_0} \varrho_0 D^{\frac{1}{2}} d^3\theta, \quad e^i = \int_{\mathcal{B}_0} \theta^i \varrho_0 D^{\frac{1}{2}} d^3\theta, \quad E^{ij} \\ &= \int_{\mathcal{B}_0} \theta^i \theta^j \varrho_0 D^{\frac{1}{2}} d^3\theta \end{aligned} \tag{14}$$

Note that all of the inertia coefficients are independent of time thus leading to a constant 12×12 mass matrix given by

$$\boldsymbol{M} = \begin{bmatrix} M_\varphi \boldsymbol{I} & e^1\boldsymbol{I} & e^2\boldsymbol{I} & e^3\boldsymbol{I} \\ e^1\boldsymbol{I} & E^{11}\boldsymbol{I} & E^{12}\boldsymbol{I} & E^{13}\boldsymbol{I} \\ e^2\boldsymbol{I} & E^{21}\boldsymbol{I} & E^{22}\boldsymbol{I} & E^{23}\boldsymbol{I} \\ e^3\boldsymbol{I} & E^{31}\boldsymbol{I} & E^{32}\boldsymbol{I} & E^{33}\boldsymbol{I} \end{bmatrix} \tag{15}$$

To determine the external force vector $\boldsymbol{F}$ in (2), we consider the virtual work of the external forces given by $\delta W = \delta\boldsymbol{q} \cdot \boldsymbol{F}$. For simplicity we assume that in addition to a body force per unit mass, $\boldsymbol{b}(\theta^i, t)$, a single force vector $\boldsymbol{f}(t)$ is applied to the material point Θ^i. Accordingly,

$$\delta W = \int_{\mathcal{B}_0} \delta\boldsymbol{x} \cdot \boldsymbol{b} \varrho_0 D^{\frac{1}{2}} d^3\theta + \delta\boldsymbol{x}(\Theta^i) \cdot \boldsymbol{f}(t) \tag{16}$$

With regard to (7), virtual displacements can be written as $\delta\boldsymbol{x} = \delta\boldsymbol{\varphi} + \theta^i \delta\boldsymbol{d}_i$. Accordingly, (16) gives rise to

$$\delta W = \delta\boldsymbol{\varphi} \cdot \boldsymbol{f}_\varphi + \delta\boldsymbol{d}_i \cdot \boldsymbol{f}^i \tag{17}$$

where the resultant force vector is given by

$$\boldsymbol{f}_\varphi = \int_{\mathcal{B}_0} \boldsymbol{b} \varrho_0 D^{\frac{1}{2}} d^3\theta + \boldsymbol{f} \tag{18}$$

and the resultant director forces assume the form

$$\boldsymbol{f}^i = \int_{\mathcal{B}_0} \theta^i \boldsymbol{b} \varrho_0 D^{\frac{1}{2}} d^3\theta + \Theta^i \boldsymbol{f} \tag{19}$$

Note that the resultant force vector $\boldsymbol{f}_\varphi$ and the resultant director forces $\boldsymbol{f}^i$ are conjugate to $\boldsymbol{\varphi}$ and the directors $\boldsymbol{d}_i$, respectively. Similar to the configuration vector (10) of the rigid body, the vector of the external forces featuring in the equations of motion (2) can be written as

$$\boldsymbol{F} = \begin{bmatrix} \boldsymbol{f}_\varphi \\ \boldsymbol{f}^1 \\ \boldsymbol{f}^2 \\ \boldsymbol{f}^3 \end{bmatrix} \tag{20}$$

The equations of motion pertaining to the rigid body can now be written in the variational form

$$\begin{aligned} &\delta\boldsymbol{\varphi} \cdot \{M_\varphi \dot{\boldsymbol{v}}_\varphi + e^i \dot{\boldsymbol{v}}_i + \boldsymbol{f}_c - \boldsymbol{f}_\varphi\} = 0 \\ &\delta\boldsymbol{d}_i \cdot \{E^{ij} \dot{\boldsymbol{v}}_j + e^i \dot{\boldsymbol{v}}_\varphi + \boldsymbol{f}^i_c - \boldsymbol{f}^i\} = 0 \end{aligned} \tag{21}$$

Here, $\boldsymbol{f}_c$ and $\boldsymbol{f}^i_c$ stand for the constraint forces and the constraint director forces, respectively. For the free rigid body, $\boldsymbol{f}_c = \boldsymbol{0}$. The specific form of the constraint director forces will be dealt with in the sequel.

3.1. Rigid body constraints

The rigid body assumption can be incorporated into the present formulation by excluding deformation of the director triad $\{\boldsymbol{d}_i\}$. This goal can be achieved by providing the following six constraint functions

$$\begin{aligned} &g_1 = \frac{1}{2}(\boldsymbol{d}_1 \cdot \boldsymbol{d}_1 - c_1) \quad g_2 = \frac{1}{2}(\boldsymbol{d}_2 \cdot \boldsymbol{d}_2 - c_2) \quad g_3 = \frac{1}{2}(\boldsymbol{d}_3 \cdot \boldsymbol{d}_3 - c_3) \\ &g_4 = \boldsymbol{d}_1 \cdot \boldsymbol{d}_2 - c_4 \quad g_5 = \boldsymbol{d}_1 \cdot \boldsymbol{d}_3 - c_5 \quad g_6 = \boldsymbol{d}_2 \cdot \boldsymbol{d}_3 - c_6 \end{aligned} \tag{22}$$

where c_i ($i = 1,\ldots,6$) are constant parameters to be specified in the reference configuration. The corresponding constraint equations $g_i = 0$ have to be satisfied at all times. With regard to (4), the six independent constraints (22) determine the configuration manifold Q^{free} of the free rigid body. It is worth mentioning that the associated tangent space (5) is given by

[1] Note that the summation convention applies to lower case roman indices occurring twice in a term. They generally range from one to three.

$$T_q Q^{\text{free}} = \{\boldsymbol{v}_\varphi \in \mathbb{R}^3,\ \boldsymbol{v}_i \in \mathbb{R}^3 (i = 1,2,3) | \boldsymbol{v}_i = \boldsymbol{\omega} \times \boldsymbol{d}_i, \boldsymbol{\omega} \in \mathbb{R}^3\} \tag{23}$$

where $\boldsymbol{\omega} \in \mathbb{R}^3$ can be interpreted as angular velocity.

3.2. Balance laws

Next we elaborate on the fundamental mechanical balance laws in the context of the free rigid body. First, we consider the **balance law for linear momentum**. Introducing $\delta\boldsymbol{\varphi} = \xi$, where $\xi \in \mathbb{R}^3$ is a constant vector, together with $\delta\boldsymbol{d}_i = \boldsymbol{0}$ into (21), a straightforward calculation gives

$$\frac{d}{dt}\boldsymbol{L} = \boldsymbol{f}_\varphi \tag{24}$$

Here, the total linear momentum of the rigid body is given by $\boldsymbol{L} = M_\varphi \boldsymbol{v}_\varphi + e^i \boldsymbol{v}_i$, and, as before, the right-hand side of (24) characterizes the resultant external force applied to the rigid body.

Concerning the **balance law for angular momentum**, substitute $\delta\boldsymbol{\varphi} = \xi \times \boldsymbol{\varphi}$ along with $\delta\boldsymbol{d}_i = \xi \times \boldsymbol{d}_i$ into (21) and subsequently take the sum of both equations. This procedure yields

$$\xi \cdot \left[\boldsymbol{\varphi} \times \{M_\varphi \dot{\boldsymbol{v}}_\varphi + e^i \dot{\boldsymbol{v}}_i - \boldsymbol{f}_\varphi\} + \boldsymbol{d}_i \times \left\{E^{ij}\dot{\boldsymbol{v}}_j + e^i \dot{\boldsymbol{v}}_\varphi + \boldsymbol{f}_c^i - \boldsymbol{f}^i\right\}\right] = 0 \tag{25}$$

We postulate that the constraint director forces do not contribute to the balance of angular momentum. This requirement yields the reduced form of the balance of angular momentum

$$\boldsymbol{d}_i \times \boldsymbol{f}_c^i = \boldsymbol{0} \tag{26}$$

This condition places three restrictions on the constraint director forces $\boldsymbol{f}_c^i$. Expressing the constraint director forces with respect to the director basis

$$\boldsymbol{f}_c^i = \Lambda^{ij}\boldsymbol{d}_j \tag{27}$$

condition (26) yields $\Lambda^{ij}\boldsymbol{d}_i \times \boldsymbol{d}_j = \boldsymbol{0}$. Due to the skew-symmetry of the cross product, we get the symmetry property $\Lambda^{ij} = \Lambda^{ji}$. Accordingly, there remain only six independent components Λ^{ij} for the specification of the constraint director forces. In particular, the six independent constraints (22) of rigidity yield constraint director forces of the form

$$\boldsymbol{f}_c^i = \sum_{l=1}^{6} \lambda^l \nabla_{\boldsymbol{d}_i} g_l \tag{28}$$

Combining (27) and (28), the components Λ^{ij} can be connected to the Lagrange multipliers:

$$[\Lambda^{ij}] = \begin{bmatrix} \lambda^1 & \lambda^4 & \lambda^5 \\ \lambda^4 & \lambda^2 & \lambda^6 \\ \lambda^5 & \lambda^6 & \lambda^3 \end{bmatrix} \tag{29}$$

Returning to (25) and taking into account (26), we further get

$$\xi \cdot \left[\boldsymbol{\varphi} \times \frac{d}{dt}\{M_\varphi \boldsymbol{v}_\varphi + e^i \boldsymbol{v}_i\} + \boldsymbol{d}_i \times \frac{d}{dt}\{E^{ij}\boldsymbol{v}_j + e^i \boldsymbol{v}_\varphi\} - \{\boldsymbol{\varphi} \times \boldsymbol{f}_\varphi + \boldsymbol{d}_i \times \boldsymbol{f}^i\}\right] = 0 \tag{30}$$

The last equation can be recast in the form

$$\frac{d}{dt}\boldsymbol{J} = \boldsymbol{\varphi} \times \boldsymbol{f}_\varphi + \boldsymbol{d}_i \times \boldsymbol{f}^i \tag{31}$$

where

$$\mathrm{J} = \boldsymbol{\varphi} \times \{M_\varphi \boldsymbol{v}_\varphi + e^i \boldsymbol{v}_i\} + \boldsymbol{d}_i \times \{E^{ij}\boldsymbol{v}_j + e^i \boldsymbol{v}_\varphi\} \tag{32}$$

is the total angular momentum of the rigid body with respect to the origin of the inertial frame of reference. The right-hand side of (31) equals the resultant external torque about the origin. Note that

$$\boldsymbol{d}_i \times \boldsymbol{f}^i = \boldsymbol{m} \tag{33}$$

can be identified as the resultant external torque relative to the point of reference of the rigid body.

We eventually turn to the **balance of energy**. Substituting $\boldsymbol{v}_\varphi$ for $\delta\boldsymbol{\varphi}$ and $\boldsymbol{v}_i$ for $\delta\boldsymbol{d}_i$, (21) leads to

$$\begin{aligned} \boldsymbol{v}_\varphi \cdot \{M_\varphi \dot{\boldsymbol{v}}_\varphi + e^i \dot{\boldsymbol{v}}_i\} &= \boldsymbol{f}_\varphi \cdot \boldsymbol{v}_\varphi \\ \boldsymbol{v}_i \cdot \{E^{ij}\dot{\boldsymbol{v}}_j + e^i \dot{\boldsymbol{v}}_\varphi\} &= \boldsymbol{f}^i \cdot \boldsymbol{v}_i - \boldsymbol{f}_c^i \cdot \boldsymbol{v}_i \end{aligned} \tag{34}$$

Note that the director velocities have to belong to the tangent space (23). This implies the relationship $\boldsymbol{v}_i = \boldsymbol{\omega} \times \boldsymbol{d}_i$, where $\boldsymbol{\omega} \in \mathbb{R}^3$ is the angular velocity. Accordingly,

$$\boldsymbol{f}_c^i \cdot \boldsymbol{v}_i = \boldsymbol{f}_c^i \cdot (\boldsymbol{\omega} \times \boldsymbol{d}_i) = \boldsymbol{\omega} \cdot \left(\boldsymbol{d}_i \times \boldsymbol{f}_c^i\right) = \boldsymbol{0} \tag{35}$$

where condition (26) has been used. The last equation conveys the well-known fact that constraint forces are workless. Taking the sum of both equations in (34) yields the balance of energy

$$\frac{d}{dt}T = P^{\text{ext}} \tag{36}$$

where

$$P^{\text{ext}} = \boldsymbol{f}_\varphi \cdot \boldsymbol{v}_\varphi + \boldsymbol{f}^i \cdot \boldsymbol{v}_i \tag{37}$$

denotes the power of the external forces acting on the rigid body. It is worth noting that the last equation can also be written in the form

$$P^{\text{ext}} = \boldsymbol{f}_\varphi \cdot \boldsymbol{v}_\varphi + \boldsymbol{m} \cdot \boldsymbol{\omega} \tag{38}$$

where the relationship $\boldsymbol{v}_i = \boldsymbol{\omega} \times \boldsymbol{d}_i$ along with definition (33) of the resultant external torque relative to the point of reference of the rigid body have been used.

3.3. Application of external torques

It can be concluded from (38) that the resultant external torque $\boldsymbol{m}$ is conjugate to the angular velocity $\boldsymbol{\omega}$. In contrast to that, the formulation in terms of natural coordinates relies on the resultant external director forces $\boldsymbol{f}^i$ which are conjugate to the director velocities $\boldsymbol{v}_i$, see (37). Using natural coordinates the question arises how the application of external torques can be realized. To answer this question we start with the kinematic relationship $\boldsymbol{v}_i = \boldsymbol{\omega} \times \boldsymbol{d}_i$ and calculate

$$\boldsymbol{d}^i \times \boldsymbol{v}_i = \boldsymbol{d}^i \times (\boldsymbol{\omega} \times \boldsymbol{d}_i) = \{(\boldsymbol{d}^i \cdot \boldsymbol{d}_i)\boldsymbol{I} - \boldsymbol{d}_i \otimes \boldsymbol{d}^i\}\boldsymbol{\omega} = 2\boldsymbol{\omega} \tag{39}$$

Using this result, the work done by the external torque $\boldsymbol{m}$ can be written as

$$\boldsymbol{m} \cdot \boldsymbol{\omega} = \frac{1}{2}\boldsymbol{m} \cdot (\boldsymbol{d}^i \times \boldsymbol{v}_i) = \frac{1}{2}\boldsymbol{v}_i \cdot (\boldsymbol{m} \times \boldsymbol{d}^i) \tag{40}$$

Since, with regard to (37), the corresponding work expression in terms of natural coordinates is given by $\boldsymbol{v}_i \cdot \boldsymbol{f}^i$, the external director forces assume the form

$$\boldsymbol{f}^i = \frac{1}{2}\boldsymbol{m} \times \boldsymbol{d}^i \tag{41}$$

This expression can be used to realize the application of an external torque $\boldsymbol{m}$. We refer to Section 6.2 for further details.

4. Kinematic pairs in the rotationless formulation

We next illustrate the formulation of kinematic pairs with the example of a cylindrical pair (Fig. 2). To this end we consider two rigid bodies formulated in terms of natural coordinates as outlined in Section 3. Accordingly, the configuration of the two-body system under consideration is characterized by redundant coordinates

$$\boldsymbol{q} = \begin{bmatrix} {}^1\boldsymbol{q} \\ {}^2\boldsymbol{q} \end{bmatrix} \quad \text{where} \quad {}^\alpha\boldsymbol{q} = \begin{bmatrix} {}^\alpha\boldsymbol{\varphi} \\ {}^\alpha\boldsymbol{d}_1 \\ {}^\alpha\boldsymbol{d}_2 \\ {}^\alpha\boldsymbol{d}_3 \end{bmatrix} \tag{42}$$

Note that the contribution of body α to the configuration vector coincides with (10). The equations of motion pertaining to the constrained mechanical system at hand can again be formulated as outlined in Section 2. Similar to (42), the contribution of each rigid body to the external forces leads to the system vector

$$\boldsymbol{F} = \begin{bmatrix} {}^1\boldsymbol{F} \\ {}^2\boldsymbol{F} \end{bmatrix} \quad \text{where} \quad {}^\alpha\boldsymbol{F} = \begin{bmatrix} {}^\alpha\boldsymbol{f}_\varphi \\ {}^\alpha\boldsymbol{f}^1 \\ {}^\alpha\boldsymbol{f}^2 \\ {}^\alpha\boldsymbol{f}^3 \end{bmatrix} \tag{43}$$

Note that the force vector ${}^\alpha\boldsymbol{F}$ associated with body α coincides with (10).

4.1. Initialization of kinematic relationships

To describe the motion of the second body relative to the first one we introduce orthonormal body-fixed triads $\{{}^\alpha\boldsymbol{d}'_i\}$ in such a way that the unit vectors ${}^\alpha\boldsymbol{d}'_3$ are parallel to the axis of the cylindrical pair (Fig. 2). Moreover, we choose the two orthonormal triads to coincide in the initial configuration, i.e. ${}^1\boldsymbol{d}'_i(0) = {}^2\boldsymbol{d}'_i(0)$. The connection between the newly introduced orthonormal triads $\{{}^\alpha\boldsymbol{d}'_i\}$ and the original triads $\{{}^\alpha\boldsymbol{d}_i\}$ (i.e. the natural coordinates) is given by

$${}^\alpha\boldsymbol{R}' = {}^\alpha\boldsymbol{F}\ {}^\alpha\boldsymbol{\Lambda}_0 \tag{44}$$

where

$${}^\alpha\boldsymbol{F} = {}^\alpha\boldsymbol{d}_i \otimes \boldsymbol{e}^i \quad \text{and} \quad {}^\alpha\boldsymbol{R}' = {}^\alpha\boldsymbol{d}'_i \otimes \boldsymbol{e}^i \tag{45}$$

The constant tensors ${}^\alpha\boldsymbol{\Lambda}_0$ in (44) are calculated in the initial configuration via

$${}^\alpha\boldsymbol{\Lambda}_0 = {}^\alpha\boldsymbol{F}^{-1}(0)\,{}^\alpha\boldsymbol{R}'(0) \tag{46}$$

The origin of the newly introduced orthonormal triads $\{{}^\alpha\boldsymbol{d}'_i\}$ is fixed at material points ${}^\alpha\Theta^i$ whose placement in the current configuration ${}^\alpha\mathcal{B}_t$ of rigid body α is denoted by ${}^\alpha\boldsymbol{\varphi}'$. Accordingly, making use of the rigid body kinematics (7),

$${}^\alpha\boldsymbol{\varphi}' = {}^\alpha\boldsymbol{\varphi} + {}^\alpha\Theta^i\ {}^\alpha\boldsymbol{d}_i \tag{47}$$

Note that the location of the material points ${}^\alpha\Theta^i$ has to be specified during initialization.

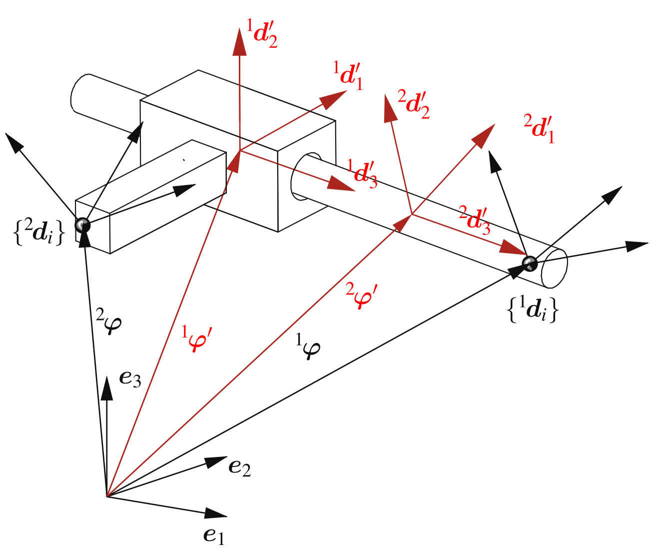

Fig. 2. Sketch of the cylindrical pair: natural coordinates $({}^\alpha\boldsymbol{\varphi},\{{}^\alpha\boldsymbol{d}_i\})$ characterizing the current configuration ${}^\alpha\mathcal{B}_t$ of rigid body α. The additional systems $({}^\alpha\boldsymbol{\varphi}',\{{}^\alpha\boldsymbol{d}'_i\})$ are introduced for the description of the motion of the second body relative to the first body (translation along and rotation about ${}^1\boldsymbol{d}'_3 = {}^2\boldsymbol{d}'_3$). The connection between $({}^\alpha\boldsymbol{\varphi}',\{{}^\alpha\boldsymbol{d}'_i\})$ and the natural coordinates $({}^\alpha\boldsymbol{\varphi},\{{}^\alpha\boldsymbol{d}_i\})$ is defined in the initial configuration of the multibody system.

4.2. Configuration space of the cylindrical pair

The configuration space of the cylindrical pair can be easily defined by distinguishing between internal constraints due the assumption of rigidity and external constraints due to the interconnection between the rigid bodies in a multibody system (see Betsch and Steinmann [1]). Accordingly, the present description of the cylindrical pair relies on $n = 24$ natural coordinates subject to *12* internal constraints $\boldsymbol{g}^{\text{int}}({}^\alpha\boldsymbol{q}) = \boldsymbol{0}(\alpha = 1,2)$, where $\boldsymbol{g}^{\text{int}} : \mathbb{R}^{12} \to \mathbb{R}^6$ follows from (22), and *4* external constraints associated with the constraint functions

$$\boldsymbol{g}^{\text{ext}}_{\text{P}}(\boldsymbol{q}) = \begin{bmatrix} {}^1\boldsymbol{d}'_1 \cdot ({}^2\boldsymbol{\varphi}' - {}^1\boldsymbol{\varphi}') \\ {}^1\boldsymbol{d}'_2 \cdot ({}^2\boldsymbol{\varphi}' - {}^1\boldsymbol{\varphi}') \end{bmatrix} \tag{48}$$

and

$$\boldsymbol{g}^{\text{ext}}_{\text{R}}(\boldsymbol{q}) = \begin{bmatrix} {}^1\boldsymbol{d}'_1 \cdot {}^2\boldsymbol{d}'_3 \\ {}^1\boldsymbol{d}'_2 \cdot {}^2\boldsymbol{d}'_3 \end{bmatrix} \tag{49}$$

To summarize, we have $n = 24$ coordinates subject to $m = 16$ constraints which can be assembled in the constraint function $\boldsymbol{g}^{\text{C}} : \mathbb{R}^{24} \to \mathbb{R}^{16}$ given by

$$\boldsymbol{g}^{\text{C}}(\boldsymbol{q}) = \begin{bmatrix} \boldsymbol{g}^{\text{int}}({}^1\boldsymbol{q}) \\ \boldsymbol{g}^{\text{int}}({}^2\boldsymbol{q}) \\ \boldsymbol{g}^{\text{ext}}_{\text{P}}(\boldsymbol{q}) \\ \boldsymbol{g}^{\text{ext}}_{\text{R}}(\boldsymbol{q}) \end{bmatrix} \tag{50}$$

Consequently, the configuration space of the cylindrical pair is defined by

$$\mathrm{Q}^{\text{C}} = \{\boldsymbol{q} \in \mathbb{R}^{24} | \boldsymbol{g}^{\text{C}}(\boldsymbol{q}) = \boldsymbol{0}\} \tag{51}$$

5. Main features of the rotationless approach

Before we deal with the discretization in time we summarize main features of the rotationless formulation of flexible multibody dynamics. In this connection it is important to note that geometrically exact Cosserat models for beams and shells fit perfectly well into the present framework. In particular, if the nonlinear beam and shell formulations are discretized in space as proposed by Betsch et al. [4–6], the equations of motion pertaining to the resulting discrete mechanical systems fit into the framework outlined in Section 2. Thus the use of natural coordinates makes possible a uniform formulation of flexible multibody dynamics[2]. Main characteristics of the present approach can be summarized as follows:

1. The inertia parameters are always constant leading to the simple structure of the inertia terms in the equations of motion (see Section 2). In particular, the differential part of the equations of motion can be written as

$$\boldsymbol{M}\ddot{\boldsymbol{q}} + \nabla V_\lambda(\boldsymbol{q}) - \boldsymbol{F} = \boldsymbol{0} \tag{52}$$

where the potential forces along with the constraint forces can be derived from an augmented potential function of the form

[2] The present framework comprises as well domain decomposition problems (see Hesch and Betsch [19]) and large deformation contact (see Hesch and Betsch [20–22]).

$$V_\lambda(\boldsymbol{q}) = U(\boldsymbol{q}) + \sum_{l=1}^{m} \lambda^l \nabla g_l(\boldsymbol{q}) \tag{53}$$

For example, the potential function $U(\boldsymbol{q})$ can be associated with the action of gravitational forces or with the deformation of flexible bodies such as nonlinear beams and shells relying on hyperelastic constitutive laws.

2. The configuration vector the complete flexible multibody systems is composed of vectors $\boldsymbol{q}_I \in \mathbb{R}^3$ and thus given by

$$\boldsymbol{q} = \begin{bmatrix} \boldsymbol{q}_1 \\ \boldsymbol{q}_2 \\ \vdots \\ \boldsymbol{q}_{\mathcal{N}} \end{bmatrix} \tag{54}$$

where $\mathcal{N}$ denotes the total number of 3-vectors $\boldsymbol{q}_I$ needed to describe a specific multibody system. Accordingly, in total, the configuration vector $\boldsymbol{q} \in \mathbb{R}^n$ has $n = 3\mathcal{N}$ components.

3. The total angular momentum of the flexible multibody systems can be cast in the form

$$\boldsymbol{J} = \sum_{a,b=1}^{\mathcal{N}} M^{ab} \boldsymbol{q}_a \times \boldsymbol{v}_b \tag{55}$$

where M^{ab} contain the constant inertia parameters and $\boldsymbol{v}_b = \dot{\boldsymbol{q}}_b$.

4. The balance of angular momentum can be written as

$$\frac{d}{dt}\boldsymbol{J} = \sum_{a=1}^{\mathcal{N}} \boldsymbol{q}_a \times (\boldsymbol{F}^a - \nabla_{\boldsymbol{q}_a} V_\lambda(\boldsymbol{q})) \tag{56}$$

Needless to say that these features have a strong impact on the discretization in time.

6. Structure-preserving discretization in time

In this section we comment on the time integration method applied to the constrained mechanical systems at hand. The specific structure-preserving scheme is second-order accurate and relies on previous works by Betsch and Steinmann [23] and Gonzalez [24]. If the underlying mechanical system is conservative, the present integrator conserves the total energy of the system. In addition to that, if the system has symmetry, the present scheme conserves the associated momentum map. We won't dwell on the algorithmic conservation properties in the present work. Instead, we focus on the implications of natural coordinates for the numerical time integration.

Consider a representative time interval $[t_n, t_{n+1}]$ with time step $\Delta t = t_{n+1} - t_n$, and given state-space coordinates $\boldsymbol{q}_n \in Q$ and $\boldsymbol{v}_n \in \mathbb{R}^n$ at time t_n. Concerning the initial values at t_0 we assume $\boldsymbol{q}_0 \in Q$ and $\boldsymbol{v}_0 \in T_q Q$. The resulting algebraic problem to be solved is stated as follows: Find $(\boldsymbol{q}_{n+1}, \boldsymbol{v}_{n+1}) \in \mathbb{R}^n \times \mathbb{R}^n$ and $\boldsymbol{\lambda}_{n,n+1} \in \mathbb{R}^m$ as the solution of the algebraic system of equations

$$\begin{aligned}
&\boldsymbol{q}_{a_{n+1}} - \boldsymbol{q}_{a_n} = \frac{\Delta t}{2}(\boldsymbol{v}_{a_n} + \boldsymbol{v}_{a_{n+1}}) \\
&\sum_{b=1}^{\mathcal{N}} M^{ab}(\boldsymbol{v}_{b_{n+1}} - \boldsymbol{v}_{b_n}) = \Delta t\left(\boldsymbol{F}^a_{n+\frac{1}{2}} - \bar{\nabla}_{\boldsymbol{q}_a} V_\lambda(\boldsymbol{q}_n, \boldsymbol{q}_{n+1})\right) \\
&\boldsymbol{g}(\boldsymbol{q}_{n+1}) = \boldsymbol{0}
\end{aligned} \tag{57}$$

for $a = 1, \ldots, \mathcal{N}$. In (57), $\bar{\nabla}_{\boldsymbol{q}_a} V_\lambda(\boldsymbol{q}_n, \boldsymbol{q}_{n+1})$ denotes a discrete derivative of the augmented potential function $V_\lambda : \mathbb{R}^n \mapsto \mathbb{R}$ in the sense of Gonzalez [25].

6.1. Rigid body constraints

Concerning the rigid body constraints dealt with in Section 3.1, we choose

$$\begin{aligned} c_1 = c_2 = c_3 = 1 \\ c_4 = c_5 = c_6 = 0 \end{aligned} \tag{58}$$

In the continuous setting this choice of parameters is equivalent to the orthonormality of the director triad $\{\boldsymbol{d}_i(t)\}$ at all times. That is, in the continuous setting, $\boldsymbol{d}_i(t) \cdot \boldsymbol{d}_j(t) = \delta_{ij}$. However, using the mid-point approximation

$$\boldsymbol{d}_{i_{n+\frac{1}{2}}} = \frac{1}{2}(\boldsymbol{d}_{i_n} + \boldsymbol{d}_{i_{n+1}}) \tag{59}$$

in general destroys the orthonormality property, although it is still satisfied at the discrete times t_n and t_{n+1} due to $(57)_3$. That is,

$$\boldsymbol{d}_{i_{n+\frac{1}{2}}} \cdot \boldsymbol{d}_{i_{n+\frac{1}{2}}} \neq \delta_{ij} \tag{60}$$

This implies that the mid-point directors represent base vectors that in general are not of unit length nor mutually orthogonal.

6.2. Consistent application of external torques

Since the rigid body formulation described in Section 3 relies on skew coordinates, property (60) does not cause any difficulties. In particular, it is obvious from (41), that the director forces due to an external torque which enter the external force vector $\boldsymbol{F}^a_{n+\frac{1}{2}}$ in $(57)_2$ are given by

$$\boldsymbol{f}^i_{n+\frac{1}{2}} = \frac{1}{2}\boldsymbol{m}_{n+\frac{1}{2}} \times \boldsymbol{d}^i_{n+\frac{1}{2}} \tag{61}$$

Here, $\boldsymbol{m}_{n+\frac{1}{2}}$ represents an external torque applied in the time interval $[t_n, t_{n+1}]$, and $\boldsymbol{d}^i_{n+\frac{1}{2}}$ are contravariant mid-point directors that can be calculated from (9) such that property

$$\boldsymbol{d}^i_{n+\frac{1}{2}} \cdot \boldsymbol{d}_{j_{n+\frac{1}{2}}} = \delta^i_j \tag{62}$$

holds. It can be easily verified that the discrete balance of angular momentum can be written as

$$\boldsymbol{J}_{n+1} - \boldsymbol{J}_n = \Delta t \sum_{a=1}^{\mathcal{N}} \boldsymbol{q}_{a_{n+\frac{1}{2}}} \times \left(\boldsymbol{F}^a_{n+\frac{1}{2}} - \bar{\nabla}_{\boldsymbol{q}_a} V_\lambda(\boldsymbol{q}_n, \boldsymbol{q}_{n+1})\right) \tag{63}$$

Note that the last equation can be viewed as discrete counterpart of the continuous version (56). If only one single rigid body is considered, (63) can be regarded as discrete counterpart of (31), where (3) has to be taken into account. Focusing on the contribution of the director forces (61) due to an external torque, for one single rigid body (63) yields

$$\begin{aligned}
\boldsymbol{J}_{n+1} - \boldsymbol{J}_n &= \Delta t \sum_{a=1}^{4} \boldsymbol{q}_{a_{n+\frac{1}{2}}} \times \boldsymbol{F}^a_{n+\frac{1}{2}} = \Delta t \boldsymbol{d}_{i_{n+\frac{1}{2}}} \times \boldsymbol{f}^i_{n+\frac{1}{2}} = \frac{\Delta t}{2} \boldsymbol{d}_{i_{n+\frac{1}{2}}} \\
&\times \left(\boldsymbol{m}_{n+\frac{1}{2}} \times \boldsymbol{d}^i_{n+\frac{1}{2}}\right) = \Delta t\left(\left(\boldsymbol{d}_{i_{n+\frac{1}{2}}} \cdot \boldsymbol{d}^i_{n+\frac{1}{2}}\right)\boldsymbol{m}_{n+\frac{1}{2}}\right. \\
&\left. - \left(\boldsymbol{d}_{i_{n+\frac{1}{2}}} \cdot \boldsymbol{m}_{n+\frac{1}{2}}\right)\boldsymbol{d}^i_{n+\frac{1}{2}}\right) = \Delta t \boldsymbol{m}_{n+\frac{1}{2}}
\end{aligned} \tag{64}$$

Consequently, formula (61) guarantees that external torques are properly applied in the discrete setting. Formula (61) has originally been proposed in Betsch et al. [26]. However this work does not rely on skew coordinates for the description of rigid bodies. Contravariant mid-point directors have been introduced in [26, Section 4.3] to remedy the lack of angular momentum consistency in the discrete setting.

7. Numerical examples

7.1. Spacecraft attitude maneuver

In the first numerical example we demonstrate the importance of formula (61) for the consistent application of external torques.

To this end we apply the present approach to the control of spacecraft rotational maneuvers.

The spacecraft is modeled as multibody system consisting of four rigid bodies (Fig. 3), namely the base body and three reaction wheels. A similar example has been dealt with in Leyendecker et al. [27]. The data for the present 4-body system have been taken from [27]. Using principal axis for each rigid body the data used in the simulations are summarized in Table 1.

The reaction wheels are spinning about body-fixed axis of the base body. For simplicity the three body-fixed axis are assumed to coincide with the director frame $\{{}^1\boldsymbol{d}_i\}$ of the base body. Spacecraft attitude maneuvers are performed by applying reaction wheel motor torques

$$ {}^2\boldsymbol{m} = (u^1)\,{}^1\boldsymbol{d}_1, \quad {}^3\boldsymbol{m} = (u^2)\,{}^1\boldsymbol{d}_2, \quad {}^4\boldsymbol{m} = (u^3)\,{}^1\boldsymbol{d}_3 \tag{65} $$

In the example we prescribe constant motor torques $u^i = 200$.

A total of $n = 48$ natural coordinates are employed to describe the multibody system at hand. Each body is subject to 6 rigid body constraints (22) and (58), giving rise to $m^{\mathrm{int}} = 24$ internal constraints. Revolute joints are used to connect the reaction wheels to the base body. This amounts to $m^{\mathrm{ext}} = 3 \times 5 = 15$ external constraints. Accordingly, in total there are $m = m^{\mathrm{int}} + m^{\mathrm{ext}} = 39$ independent constraints leading to $n - m = 9$ degrees of freedom.

The newly devised formula (61) has been used to consistently apply the motor torques to the reaction wheels. In this connection Remark 2.2 has been taken into account. That is, the torque acting on the base body is given by

$$ {}^1\boldsymbol{m} = -({}^2\boldsymbol{m} + {}^3\boldsymbol{m} + {}^4\boldsymbol{m}) \tag{66} $$

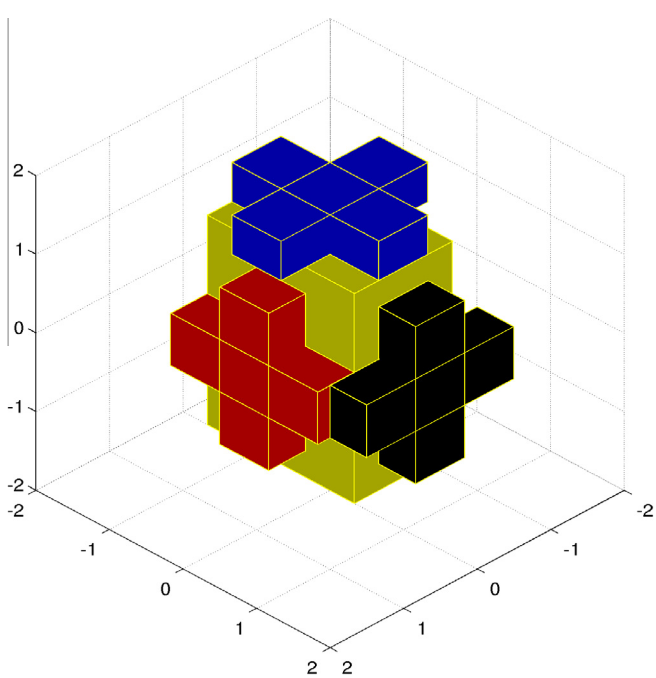

Fig. 3. The spacecraft as 4-body system.

Table 1
Spacecraft: Data for the 4-body system. Note that L denotes the distance between the center of mass of the reaction wheels and the base body.

Body	M_φ	E^{11}	E^{22}	E^{33}	L
1	1005.3096	89.3609	201.0619	357.4434	
2	424.1150	8.8357	106.0288	106.0288	0.9167
3	424.1150	106.0288	8.8357	106.0288	1.25
4	424.1150	106.0288	106.0288	8.8357	1.5833

Since no resultant external torque acts on the spacecraft, the total angular momentum is a first integral of the motion. This can be verified along the lines of Section 6.2. In particular,

$$ \begin{aligned} \boldsymbol{J}_{n+1} - \boldsymbol{J}_n &= \Delta t \sum_{a=1}^{12} \boldsymbol{q}_{a_{n+\frac{1}{2}}} \times \boldsymbol{F}^a_{n+\frac{1}{2}} = \Delta t \sum_{b=1}^{4} {}^b\boldsymbol{d}_{i_{n+\frac{1}{2}}} \times {}^b\boldsymbol{f}^i_{n+\frac{1}{2}} \\ &= \frac{\Delta t}{2} \sum_{b=1}^{4} {}^b\boldsymbol{d}_{i_{n+\frac{1}{2}}} \times \left({}^b\boldsymbol{m}_{n+\frac{1}{2}} \times {}^b\boldsymbol{d}^i_{n+\frac{1}{2}} \right) \\ &= \Delta t \sum_{b=1}^{4} \left(\left({}^b\boldsymbol{d}_{i_{n+\frac{1}{2}}} \cdot {}^b\boldsymbol{d}^i_{n+\frac{1}{2}} \right) {}^b\boldsymbol{m}_{n+\frac{1}{2}} - \left({}^b\boldsymbol{d}_{i_{n+\frac{1}{2}}} \cdot {}^b\boldsymbol{m}_{n+\frac{1}{2}} \right) {}^b\boldsymbol{d}^i_{n+\frac{1}{2}} \right) \\ &= \Delta t \sum_{b=1}^{4} {}^b\boldsymbol{m}_{n+\frac{1}{2}} = \boldsymbol{0} \end{aligned} \tag{67} $$

where use has been made of (65) and (66). In the numerical simulations we focus on the 3-component J_3 of the total angular momentum and the total kinetic energy T of the multibody system at hand. The numerical results due to the application of the newly devised formula (61) are denoted by J_3^{kontra} and T^{kontra}.

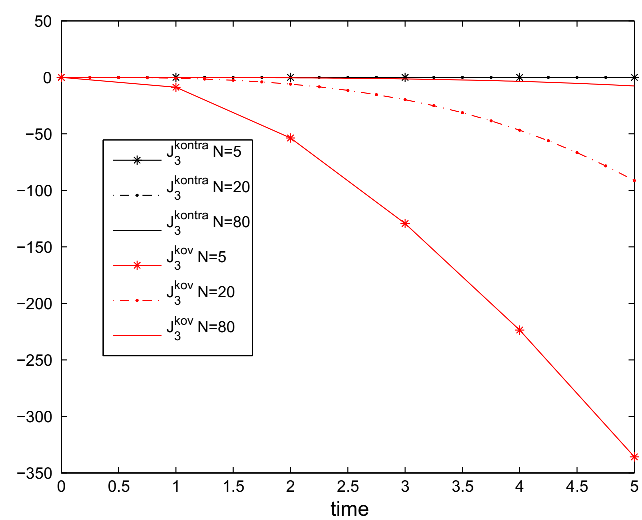

Fig. 4. Spacecraft: comparison of angular momentum.

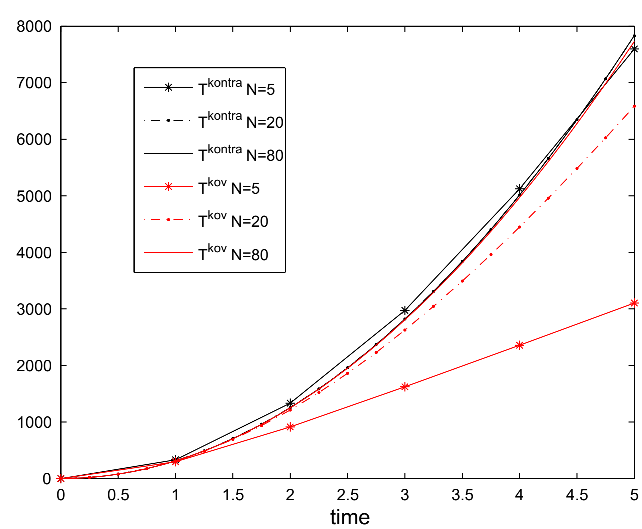

Fig. 5. Spacecraft: comparison of kinetic energy.

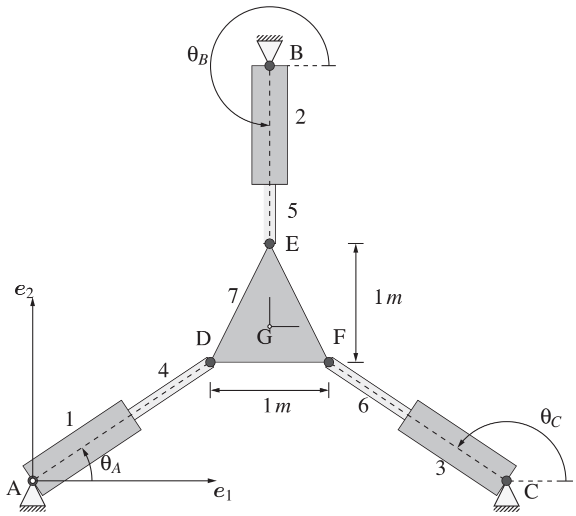

Fig. 6. The 3-RPR planar parallel robot.

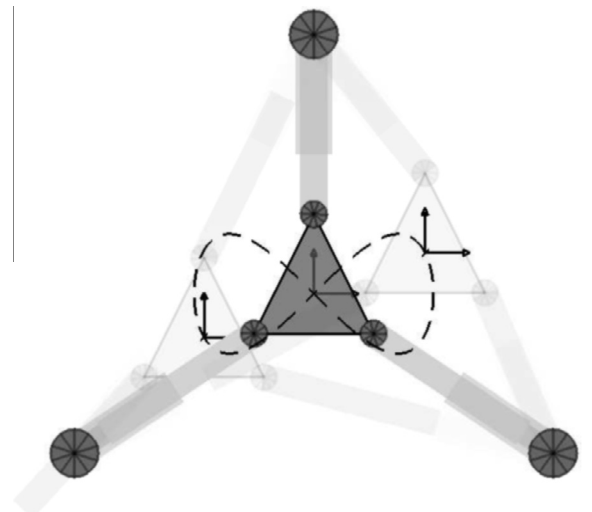

Fig. 8. Parallel robot: Final position simulated with the newly proposed method. The figure-8 trajectory is correctly tracked by the mass center of the end-effector.

Table 2
Geometry and inertia properties of the parallel robot.

Body	Width (m)	Length (m)	Mass (kg)	Moment of inertia (kg m^2)
1, 2, 3	0.3	1.0	2.4	0.218
4, 5, 6	0.1	1.5	1.2	0.226
7	1.0	1.0	0.5	0.049

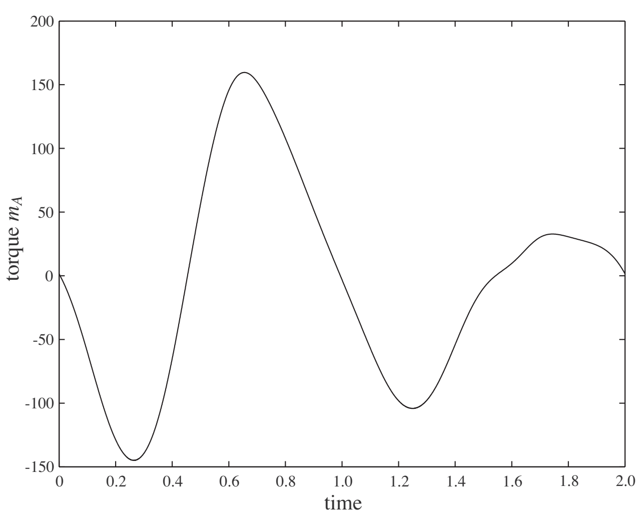

Fig. 7. Parallel robot: Driving torque at joint A determined by the inverse dynamics analysis.

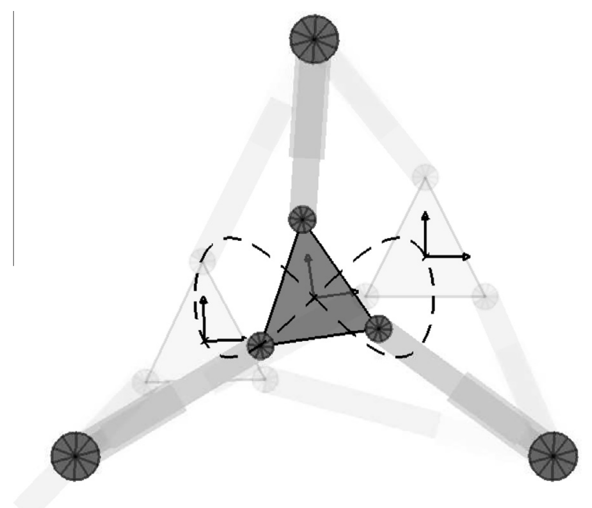

Fig. 9. Parallel robot: Final position simulated with the original method. The inconsistent application of the driving torques leads to a deviation from the correct motion.

For comparison we apply the motor torques via the straightforward mid-point evaluation of the continuous expression of the 'original' formulation (see [26])

$$\boldsymbol{f}_{i_{n+\frac{1}{2}}} = \frac{1}{2}\boldsymbol{m}_{n+\frac{1}{2}} \times \boldsymbol{d}_{i_{n+\frac{1}{2}}} \tag{68}$$

The corresponding results are denoted by J_3^{kov} and T^{kov}.

A number of N time steps is used to resolve the time interval [0, 5]. It can be observed from Fig. 4 that J_3^{kontra} stays constant for all N. This corroborates algorithmic conservation of the total angular momentum. In severe contrast to that J_3^{kov} does not stay constant. Accordingly the balance law for angular momentum is violated. This discretization error can be decreased by raising the number of time steps N. These observations are further supported by considering the total kinetic energy in Fig. 5. Accordingly, T^{kontra} does hardly change if the time steps are refined. That is, using only $N = 5$ time steps already leads to a very good approximation of the kinetic energy. This is in severe contrast to T^{kov}.

7.2. Parallel robot

In the second example we consider the planar parallel robot depicted in Fig. 6. Each of the three legs of the parallel robot consists of a prismatic kinematic pair along with two revolute joints. The parallel mechanism has three degrees of freedom and is referred to as the 3-RPR planar parallel manipulator, where the underlined letter indicates that one of the revolute joints of each leg is driven.

In the forward dynamics simulation we rely on the results of an inverse dynamics analysis due to McPhee and Redmond [28]. The goal of the inverse dynamics analysis is to determine the driving torques required to translate the center of mass G of the end-effector in a figure-8 pattern, with a cycle time of 2 s, defined by

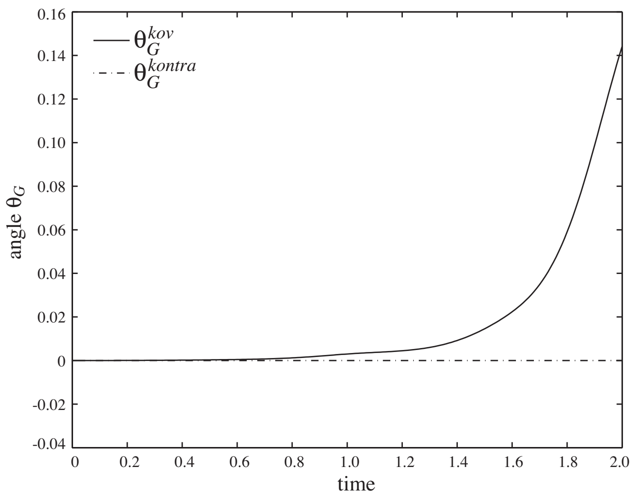

Fig. 10. Parallel robot: Rotation angle of the end-effector.

i	a_i	α_i	d_i	θ_i
0	0	0	0	0
1	0	90	310	0
2	0	−90	0	0
3	0	−90	400	0
4	0	90	0	0
5	0	90	390	0
6	0	−90	0	0
7	0	0	0	0

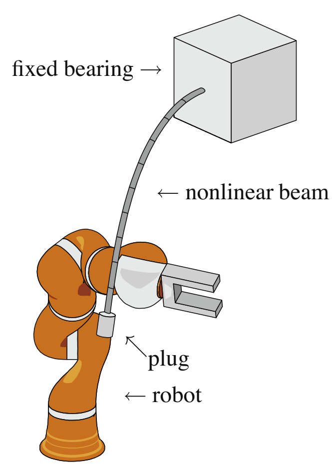

Fig. 11. Hartenberg-Denavit parameters of the lightweight robot (left) and components of the flexible multibody system (right).

$$
\begin{aligned}
x_G &= 2 + \sin(\pi t) \\
y_G &= \frac{4}{3} + \frac{1}{2}\sin(2\pi t) \\
\theta_G &= 0
\end{aligned}
\tag{69}
$$

The geometry and inertia properties of the parallel robot have been taken as well from McPhee and Redmond [28] and are summarized in Table 2. In addition to that, we remark that the position of points B and C (Fig. 6) is given by $x_B = 2$, $y_B = 3.5$, and $x_C = 4.0$. The result of the inverse dynamics analysis gives rise to the three driving torques, one of which is depicted in Fig. 7 (compare with Fig. 12 in McPhee and Redmond [28]).

Obviously, using the three driving torques from the inverse dynamics analysis in the forward dynamics simulation along with the data in Table 2 should lead to the motion of the end-effector given by (69). That is, the trajectory of the center of mass G of the end-effector should follow a figure-8 pattern, while the end-effector should not rotate.

In the simulation we use 200 time steps and apply the newly developed formula (61) for the consistent application of external torques. It can be observed from Fig. 8 that the proposed simulation method yields the correct motion. In sharp contrast to that, using instead of formula (61) the mid-point evaluation of the original formulation, Eq. (68), yields a deviation from the correct motion (Fig. 9). This observation is further supported by Fig. 10, where the rotation angle of the end-effector is plotted versus time. While the advocated method correctly reproduces the constant angle $\theta_G^{kontra} = 0$, the angle θ_G^{kov} determined by the original approach deviates significantly from the correct value. These results strongly support the need for a consistent formulation of external torques in the underlying rotationless formulation.

7.3. Lightweight robot applied to the mounting of flexible cables

The third example deals with a multibody model of the KUKA-DLR LightWeight Robot (LWR) (Bischoff et al. [29]) applied to the manipulation of highly flexible cables (Fig. 11). The LWR is modeled as multibody system with seven revolute joints. On the other hand the flexible cable is formulated as geometrically exact beam

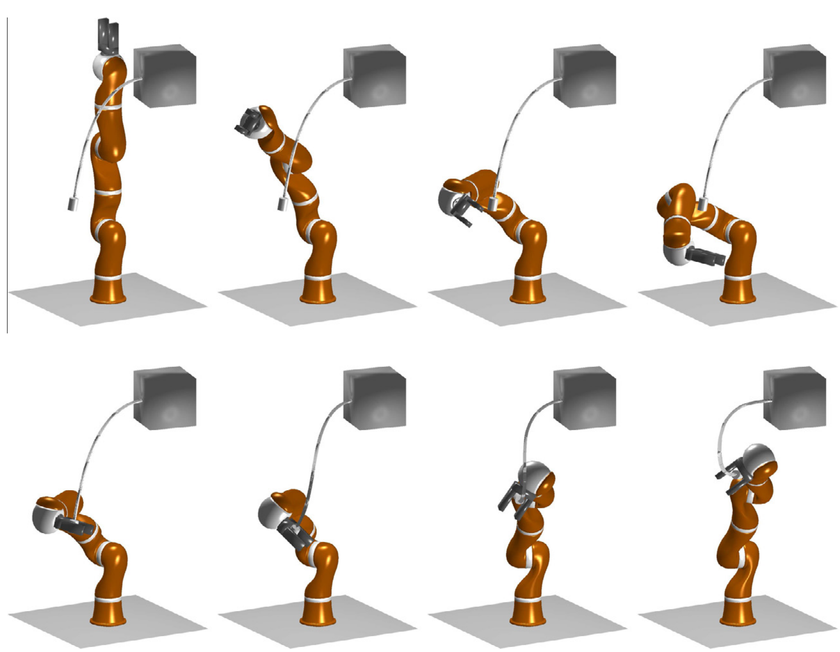

Fig. 12. Snapshots of the motion for $t \in \{0, 1, 2, 5, 6, 7, 10, 12\}$.

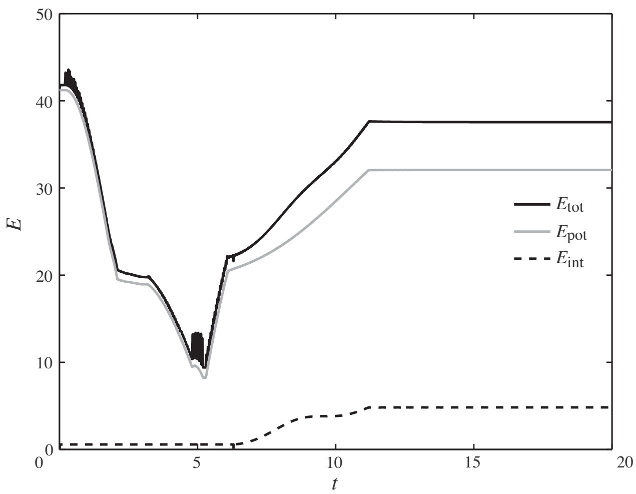

Fig. 13. Energy evolution of the flexible multibody system: total energy E_{tot}, potential energy E_{pot} and internal strain energy E_{int}.

connected to a plug which itself is modeled as rigid body. The right end of the cable is clamped to a rigid block fixed in space.

In the forward simulation the end-effector grips the plug at the left end of the cable and subsequently bends the cable leading to large deformations. The joint-torques of the LWR are prescribed by applying the approach described in Section 6.2. Snapshots of the motion are depicted in Fig. 12. In addition to that, in Fig. 13 the evolution of the total mechanical energy is shown along with the potential energy (due to gravity) and the strain energy stored in the cable.

8. Conclusions

Natural coordinates allow for a systematic description of complex multibody systems. In this connection, the specific rigid body formulation described in Section 3 provides the link between standard multibody systems comprised of rigid bodies and flexible multibody systems resulting from the rotationless finite element discretization of Cosserat solids such as shear deformable beams (Betsch and Steinmann [5]) and shells (Betsch and Sänger [6]). The rotationless approach leads to a uniform set of differential–algebraic equations governing the motion of general flexible multibody systems. Moreover, the specific structure of the equations of motion makes possible the design of structure-preserving time-stepping schemes which exhibit superior numerical stability and robustness.

On the other hand, we have shown that the rigid body formulation in terms of natural coordinates requires particular caution when it comes to applying external torques. In a previous work (Betsch et al. [26]) an ad hoc modification of the external forces has been proposed to restore the balance law for angular momentum in the discrete setting. In the present work this modification has been further substantiated by resorting to skew coordinates from the outset. It is worth noting that our approach has been guided by the theory of Cosserat points (Rubin [17]).

The numerical examples presented in Sections 7.1 and 7.2 strongly support the importance of a consistent application of external torques in the underlying rotationless formulation of multibody systems. It is obvious that the consistent formulation and numerical treatment of external torques is of crucial importance for the application of the present approach to the (optimal) control of (flexible) multibody systems.

Acknowledgments

The authors thank Christian Becker for his contribution of the simulation in Section 7.2. Support for this research was provided by the Deutsche Forschungsgemeinschaft (DFG) under Grant BE 2285/5. This support is gratefully acknowledged.

References

[1] Betsch P, Steinmann P. A DAE approach to flexible multibody dynamics. Multibody Syst Dyn 2002;8:367–91.
[2] Betsch P, Sänger N. A nonlinear finite element framework for flexible multibody dynamics: rotationless formulation and energy-momentum conserving discretization. In: Bottasso Carlo L, editor. Multibody dynamics: computational methods and applications. Computational methods in applied sciences, vol. 12. Springer-Verlag; 2009. p. 119–41.
[3] Betsch P, Steinmann P. Constrained integration of rigid body dynamics. Comput Methods Appl Mech Eng 2001;191:467–88.
[4] Betsch P, Steinmann P. Frame-indifferent beam finite elements based upon the geometrically exact beam theory. Int J Numer Methods Eng 2002;54:1775–88.
[5] Betsch P, Steinmann P. Constrained dynamics of geometrically exact beams. Comput Mech 2003;31:49–59.
[6] Betsch P, Sänger N. On the use of geometrically exact shells in a conserving framework for flexible multibody dynamics. Comput Methods Appl Mech Eng 2009;198:1609–30.
[7] Géradin M, Cardona A. Flexible multibody dynamics: a finite element approach. John Wiley & Sons; 2001.
[8] Ibrahimbegović A, Mamouri S. On rigid components and joint constraints in nonlinear dynamics of flexible multibody systems employing 3d geometrically exact beam model. Comput Methods Appl Mech Eng 2000;188:805–31.
[9] Bauchau OA. Flexible multibody dynamics. Solid mechanics and its applications, vol. 176. Springer-Verlag; 2011.
[10] Ibrahimbegović A, Mamouri S, Taylor RL, Chen AJ. Finite element method in dynamics of flexible multibody systems: Modeling of holonomic constraints and energy conserving integration schemes. Multibody Syst Dyn 2000;4(2-3):195–223.
[11] Bathe KJ. Conserving energy and momentum in nonlinear dynamics: A simple implicit time integration scheme. Comput Struct 2007;85(7–8):437–45.
[12] Leyendecker S, Marsden JE, Ortiz M. Variational integrators for constrained dynamical systems. Z Angew Math Mech (ZAMM) 2008;88(9):677–708.
[13] Betsch P, Hesch C, Sänger N, Uhlar S. Variational integrators and energy-momentum schemes for flexible multibody dynamics. J Comput Nonlinear Dyn 2010;5(3). 031001/1–11.
[14] García de Jalón J. Twenty-five years of natural coordinates. Multibody Syst Dyn 2007;18(1):15–33.
[15] Saletan EJ, Cromer AH. Theoretical mechanics. John Wiley & Sons; 1971.
[16] Uhlar S, Betsch P. A rotationless formulation of multibody dynamics: modeling of screw joints and incorporation of control constraints. Multibody Syst Dyn 2009;22(1):69–95.
[17] Rubin MB. Cosserat theories: shells rods and points. Solid mechanics and its applications, vol. 79. Kluwer Academic Publishers; 2000.
[18] Marsden JE, Ratiu TS. Introduction to mechanics and symmetry. 2nd ed. Springer-Verlag; 1999.
[19] Hesch C, Betsch P. Transient three-dimensional domain decomposition problems: Frame-indifferent mortar constraints and conserving integration. Int J Numer Methods Eng 2010;82(3):329–58.
[20] Hesch C, Betsch P. A mortar method for energy-momentum conserving schemes in frictionless dynamic contact problems. Int J Numer Methods Eng 2009;77(10):1468–500.
[21] Hesch C, Betsch P. Transient 3d contact problems–NTS method: mixed methods and conserving integration. Comput Mech 2011;48(4):437–49.
[22] Hesch C, Betsch P. Transient three-dimensional contact problems: mortar method. Mixed methods and conserving integration. Comput Mech 2011;48(4):461–75.
[23] Betsch P, Steinmann P. Conservation properties of a time FE method. Part III: Mechanical systems with holonomic constraints. Int J Numer Methods Eng 2002;53:2271–304.
[24] Gonzalez O. Mechanical systems subject to holonomic constraints: Differential-algebraic formulations and conservative integration. Phys D 1999;132:165–74.
[25] Gonzalez O. Time integration and discrete Hamiltonian systems. J Nonlinear Sci 1996;6:449–67.
[26] Betsch P, Siebert R, Sänger N. Natural coordinates in the optimal control of multibody systems. J Comput Nonlinear Dyn 2012;7(1):011009/1–8.
[27] Leyendecker S, Ober-Blöbaum S, Marsden JE, Ortiz M. Discrete mechanics and optimal control for constrained systems. Optim Control Appl Methods 2010;31(6):505–28.
[28] McPhee JJ, Redmond SM. Modelling multibody systems with indirect coordinates. Comput Methods Appl Mech Eng 2006;195:6942–57.
[29] Bischoff R, Kurth J, Schreiber G, Koeppe R, Albu-Schäffer A, Beyer A, Eiberger V, Haddadin S, Stemmer A, Grunwald G, Hirzinger G. The KUKA-DLR lightweight robot arm – a new reference platform for robotics research and manufacturing. In: Robotics (ISR), 2010 41st international symposium on and 2010 6th german conference on robotics (ROBOTIK);2010. p. 1–8.